SCALING EFFECTS IN THE LOW VELOCITY IMPACT RESPONSE OF CFRP LAMINATES

Z.W. Xu[1], F.J. Yang[1], Z.W, Guan[1,2] and W.J. Cantwell[3]

[1] School of Engineering, University of Liverpool, United Kingdom
[2] School of Civil & Transport Engineering, South China University of Technology, China
[3] Department of Aerospace Engineering, Khalifa University, United Arab Emirates

Keywords: Scaling effects, Size effects, Low velocity impact, Composite laminates

ABSTRACT

Scaling effects in the impact response of a carbon fibre-reinforced polymer (CFRP) composite have been investigated through experimental tests conducted on an instrumented drop-weight tower at five different impact energies, including an impact energy just greater than that is required to perforate the CFRP laminates. An examination of the tested composite panels highlighted that the predominant failure mechanism was fibre fracture extending away from the centre of the panel in warp and weft directions. In addition, it has been shown by analysing the load-displacement traces that the elastic response obeys a simple scaling law, whereas impact damage does not scale in accordance with simple scaling laws, with damage becoming more severe in the large panels. Such effects, i.e. the presence of increased severity of damage in the larger scale sizes, has been explained from the perspective of the normalised projectile displacement in the fibre fracture phase, the normalised crack length and the absorbed energy in the impact event. It is argued that the energy absorbed in fibre fracture phase does not scale in the expected manner, leading to greater levels of fibre damage in the larger plates. Further, the "unexpected" lower level of fibre fracture in the scaled panels subjected to the impact energy higher than the perforation energy threshold has been explained a result of the development of some degree of matrix crushing failure and delamination during the impact event.

1 INTRODUCTION

Thanks to their lightweight nature, fibre-reinforced polymers (FRPs) have been increasingly utilised for large load-bearing structures in the aerospace and marine industries. Using these lightweight materials often necessitates extensive experimental validations on full-scale prototypes. To save time and financial costs, these full-scale prototype validations are frequently replaced by testing on small-scale laboratory specimens or models that are determined by applying the principles of similitude (i.e. dimensional analysis). However, a concern of using small-scale model validation is that the response of the full-scale model may not be truly represented by that of the corresponding small-scale model, due to scaling effects. For example, FRP composite structures generally exhibit a decreased strength with increasing geometry size [1, 2]. Thus, to ensure the successful and cost-effective design of composite structures, it is critical to identify scaling effects in the mechanical response such that the behaviour of the full-scale structure can be predicted by extrapolating from that of the small-scale model.

Research on this topic initially focused on understanding size effects in the unnotched strength of composites. Based on the Buckingham-Π theorem [3], tests were designed and conducted by Wisnom [4] and Kellas *et al* [5-7] on carbon fibre-reinforced polymer (CFRP) laminates, highlighting significant scaling effects in the tensile, compressive and flexural strength values. Given that composite structures are very susceptible to notches, which are the primary sites of stress concentration and damage initiation, attention has also been paid to investigating scaling effects in the notched strength of composite structures [8-13]. In the scaling tests conducted for open-hole composite specimens, Wisnom and co-workers [9] observed that the notched strength of this type of composites is dependent on scale size.

As a result of the increasing possibility of composite structures being subjected to dynamic loading scenarios, there has been a growing interest in investigating scaling effects in the impact response of

composite structures. Morton [14] conducted a number of impact tests on unidirectional CFRP laminates with different stacking sequences, observing that the strength under impact increased significantly with decreasing specimen size. It was also noted that the impact contact time should scale linearly with the scaling factor, while the impact force should scale as the scaling factor squared. Swanson [15] performed scaling tests on a large number of CFRP plates and cylinders subjected to drop-weight and airgun impact. It was revealed that both the strength and failure strain of the composites were insensitive to specimen size, whereas the severity of delamination showed a significant dependency on scale size. Detailed studies have also been conducted on fibre-metal composite structures and CFRP-skin sandwich structures [16-19] subjected to quasi-static and low velocity impact loading conditions. In these studies, no significant scaling effects in the quasi-static responses of both types of material were observed. Similarly, under impact conditions, the impact force, maximum deflection and damage threshold energy were found to be size independent.

An examination of the published studies on scaling effects in the response of composite structures indicates that most of them have been based on unidirectional composites rather than textile composites, despite the fact that the later offer many advantages, such as improved notched sensitivity, superior impact resistance and lower fabrication costs. It is also evident that very little work has been conducted at energies above that required to perforate the composite target. Clearly, identifying this energy threshold is of significance for composite structures designed to protect personnel during impact loading scenarios such as blast and explosions. The aim of this work is, therefore, to experimentally study scaling effects in plain woven CFRP laminates subjected to impact loading conditions up to and beyond the perforation threshold.

2 SIMILITUDE APPROACH

In this study, the similitude approach utilised defines a geometrically-similar scaling law that can be used for predicting the response parameters based on a set of appropriately-selected input parameters, which can be further categorised into geometrical, material and additional parameters. In geometrical input parameters, a length term, L, and a thickness term, h, are defined to determine the sizes of each scaled specimen. Material input parameters generally include the elastic properties (e.g. Young's modulus) and the density of the composite material. Additional input parameters are used to characterise testing conditions such as the loading velocity, the diameter of the projectile and the size of the support. The output or response parameters include the maximum, central deflection of specimen, the measured contact force, the duration of contact and the load-deflection response. Table 1 summarises all the input and output parameters, as well as their dependencies on the scaling factor, n, which is a defined as the ratio of a characteristic length in the scaled model to that in the full-scale structure [20]. When undertaking scaling tests of this nature, the impact mass must be scaled as n^3, producing the same impact velocity in all scaling tests.

Parameter	Dependency
Panel length	n
Panel thickness	n
Projectile diameter	n
Support inner diameter	n
Impact mass	n^3
Impact energy	n^3
Impact contact duration	n
Maximum impact force	n^2
Target displacement	n
Damage area	n^2

Table 1: Model parameters and their dependencies on the scaling factor [20]

3 EXPERIMENTAL PROCEDURE

3.1 Material description

All specimens used in this study were fabricated from EP121-C15-53, a prepreg supplied by Gurit Ltd [21]. This prepreg system is based on a plain woven fabric pre-impregnated with 53% EP121 epoxy resin. The woven fabric is made from 3k HTA 40 carbon fibres and has an areal density of 193 g/m^2 (±5%). The epoxy resin is a highly toughened system and can be cured at temperatures between 120 and 160 ℃. This prepreg has a nominal thickness of 0.28 mm in its as-supplied form. All the laminated specimens were initially prepared at room temperature using a hand lay-up technique and then cured with a hot-press at a constant pressure of 2 bar and a dwell temperature of 135 °for 70 minutes before cooling. Four scaled sizes of specimen, referred to as 1/4, 1/2, 3/4 and 1 (full scale), were fabricated based on 4, 8, 12 and 16 layers of the prepreg respectively, as shown in Figure 1.

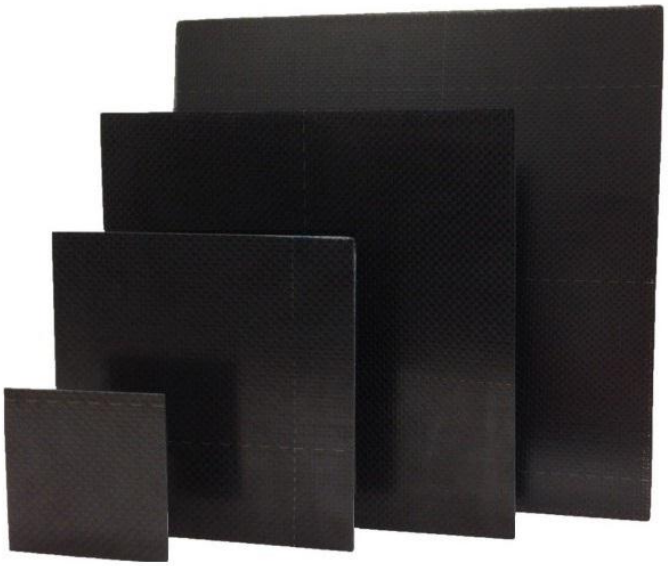

Figure 1: Photos of the four scaled sizes of composite panel

3.2 Details of tests

To investigate scaling effects in the impact response of this composite system, five sets of tests were undertaken on the instrumented drop-weight test set-up schematically shown in Figure 2. The five sets of tests were conducted at impact energies of $67.46n^3$, $97.22n^3$, $128.4n^3$, $148.8n^3$ and $170.7n^3$ Joules, respectively. Here, the first four impact energies were used to produce different levels of damage in the composite panels without being perforated, whereas the last impact energy was selected to be just greater than that required to fully perforate the panels. Each set of tests were further comprised of four scaled test cases, i.e. n=1/4, n=1/2, n=3/4 and n=1, the detailed configurations of which are given in Table 2.

In each test case, the scaled CFRP panel, which has dimensions of $260n \times 260n \times 4.48n$ mm, was placed on a support ring with an inner diameter of $200n$ mm. The simply supported panel was then transversely impacted at the centre by a projectile with a diameter of $20n$ mm. A mass carriage with some weights was attached above the projectile, forming a required amount of impact mass or energy. It should be noted that in all tests the projectile was released from the same height, i.e. 500 mm, to give a constant impact velocity of approximately 3.13 m/s in all tests. Given that the same impact velocity was applied, the impact masses corresponding to the five sets of tests were determined as $13.77n^3$, $19.84n^3$, $26.20n^3$, $30.37n^3$ and $34.84n^3$ kg respectively, using the following equation:

$$M_n = \frac{E_n}{gH} \tag{1}$$

where M_n and E_n are the impact mass and energy corresponding to the scaling factor n, g is a constant representing the acceleration of gravity, and H stands for the release height of the projectile.

During the impact event, the load-time history was recorded using a Kistler 9021A piezo-electric load cell connected to the projectile, while the movement of the projectile and the deformation of the specimen were captured using a high-speed camera positioned in front of the drop-weight tower. High-speed footage was recorded and the resulting images were analysed after the test using the motion analysis software ProAnalyst to obtain the displacement-time history, which was ultimately combined with the load-time history to derive the load-displacement response.

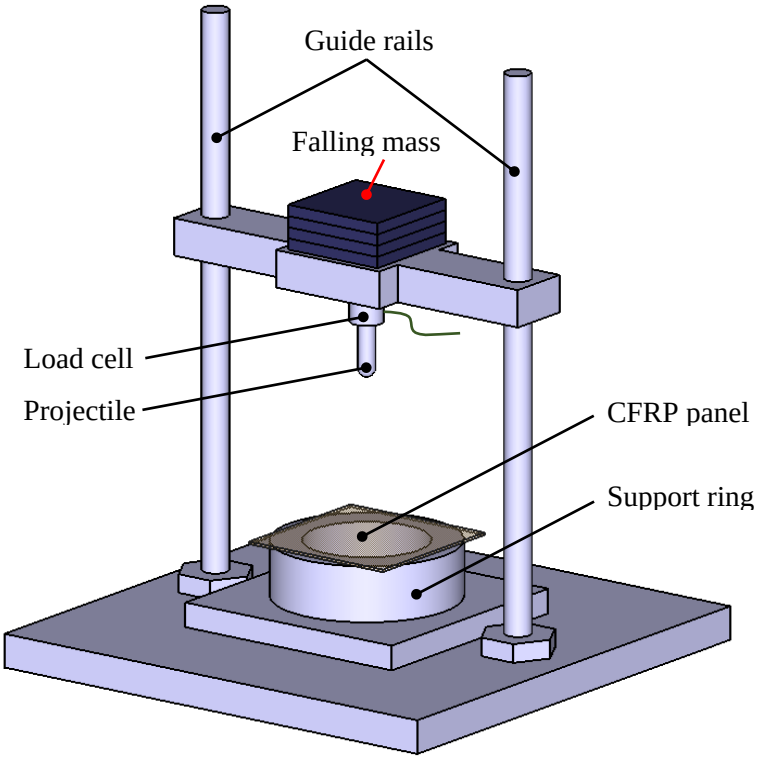

Figure 2: Schematic of the instrumental drop-weight test set-up

Scale n	Length (mm)	Thickness (mm)	No. of plies	Projectile diameter (mm)	Support inner diameter (mm)	Drop height (mm)
1/4	65	1.12	4	5	50	500
1/2	130	2.28	8	10	100	500
3/4	195	3.36	12	15	150	500
1	260	4.48	16	20	200	500

Table 2: Summary of specimen configurations and test conditions

4 RESULTS AND DISCUSSION

Figure 3a shows the load-displacement traces obtained following impact tests on the four scaled sizes of panels at an energy of $97.22n^3$ Joules. As is evident from this figure, all four traces show similar trends, with the load increasing to a maximum before plateauing at an approximately constant value force, followed by a rapid decrease of the load with decreasing deflection, due to the resilience of the panel. A subsequent examination of the impacted panels highlighted the presence of fibre fracture extending from the centre of the panel in both the warp and weft directions, as shown in Figure 4. It is

also highlighted that no significant delamination occurred during the impact event, as demonstrated in one of the sectioned panels shown in Figure 5. Given that the dominant failure mode in these panels is fibre fracture rather than delamination, it is believed that the maximum force in the load-displacement curve coincides with the initiation of lower surface fibre fracture and that the subsequent plateau is associated with the progression of fibre fracture.

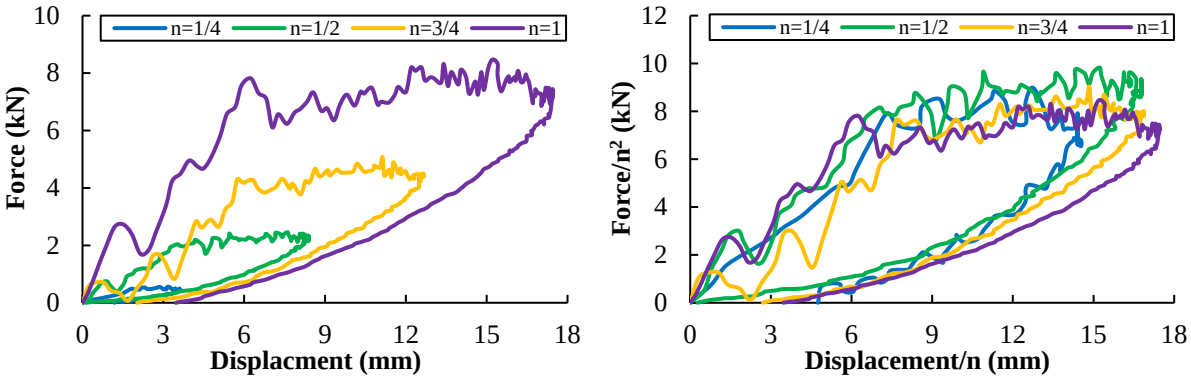

(a) Original traces (b) Normalised traces

Figure 3: Load-displacement traces following impact tests at an energy of $97.22n^3$ Joules

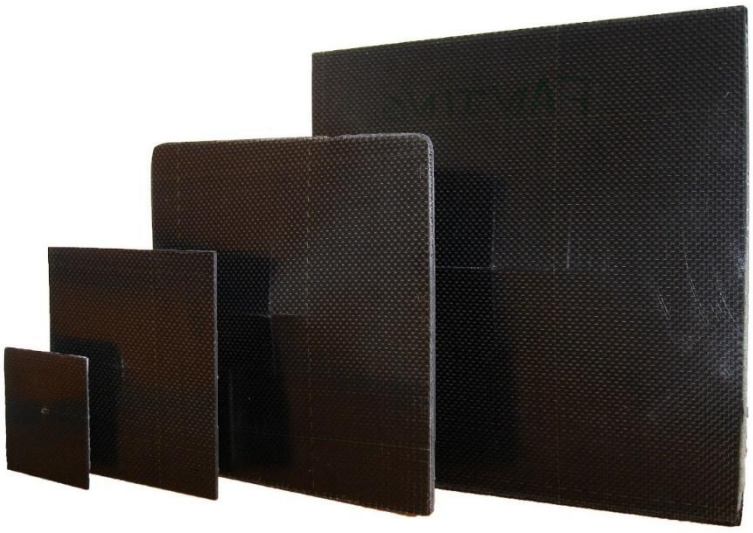

Figure 4: Failure modes of the scaled panels in the first four sets of tests

Figure 5: Typical cross-section in the damaged panels in the first four sets of tests

To better investigate scaling effects in the impact response, the load-displacement traces in Figure 3a were normalised by dividing the load by n^2 and the displacement by n. The resulting data, as shown in Figure 3b, seemingly suggest that the impact response of this type of material complies with simple

scaling laws, as the four normalised traces are found to be in a reasonable degree of agreement between each other. However, a closer examination indicates that impact damage does not obey a simple scaling law, with the severity of damage increasing in the larger panels. This effect will be quantitatively addressed later from three points of view, i.e. the length of fibre fracture phase, the physical length of the crack, and the energy absorbed during the impact event.

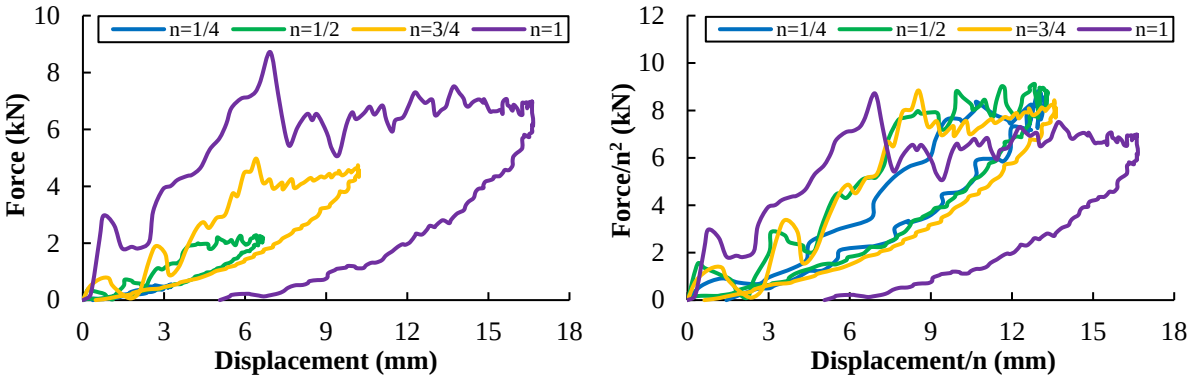

(a) Original traces (b) Normalised traces

Figure 6: Load-displacement traces following impact tests at an energy of $67.46n^3$ Joules

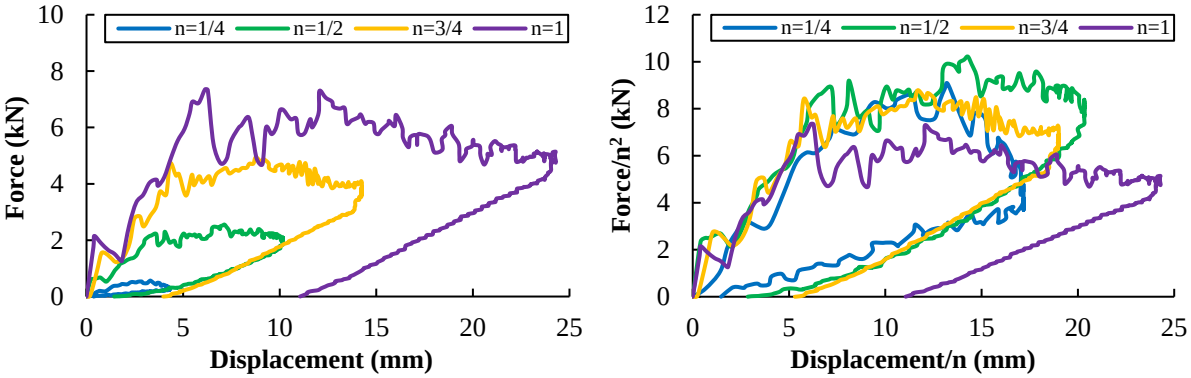

(a) Original traces (b) Normalised traces

Figure 7: Load-displacement traces following impact tests at an energy of $128.4n^3$ Joules

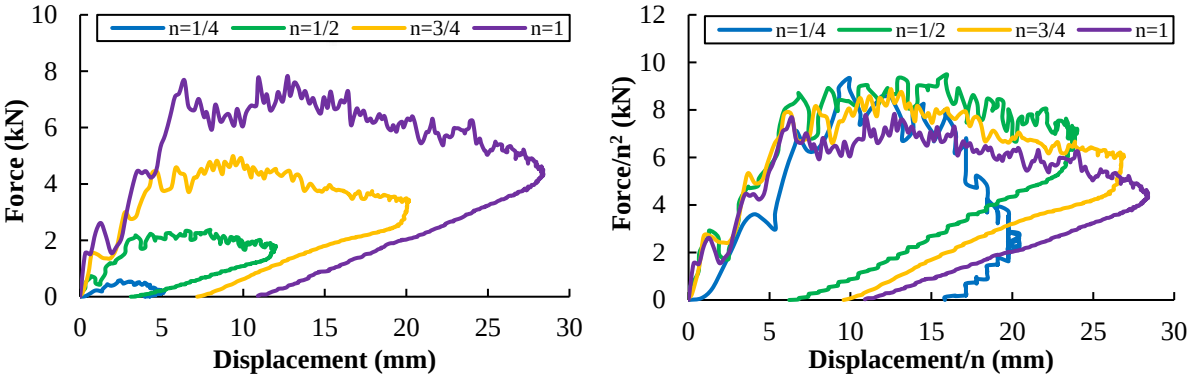

(a) Original traces (b) Normalised traces

Figure 8: Load-displacement traces following impact tests at an energy of $148.8n^3$ Joules

Figures 6-8 show the original and normalised load-displacement traces derived following tests at impact energies of $67.46n^3$, $128.4n^3$ and $148.8n^3$ Joules, respectively. For each impact energy, the original load-displacement traces again exhibit similar responses, with the load increasing to a maximum

point (associated with the initiation of fibre fracture) followed by a highly oscillatory region (associated with the propagation of fibre fracture). From the normalised data, it is seen that the elastic phase of all traces tends to coincide, while the subsequent force plateau shows a strong dependency on scale size, again suggesting that simple scaling laws do not apply for this type of material.

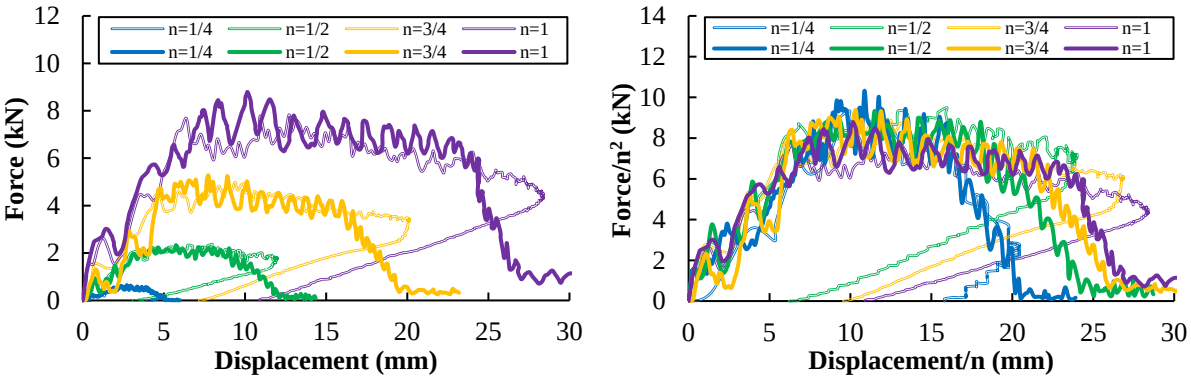

(a) Original traces (b) Normalised traces

Figure 9: Load-displacement traces following impact tests at an energy of $170.7n^3$ Joules (the results corresponding to impact tests at an energy of $148.8n^3$ Joules are included using hollow lines)

Figure 9a shows the load-displacement traces obtained following impact tests at an energy of $170.7n^3$ Joules, an energy that is just greater than that needed to perforate the panels. Here, the results of impact tests at an energy of $148.8n^3$ Joules are included using hollow lines for comparison. It is evident that the traces corresponding to an energy of $170.7n^3$ Joules exhibit similar trends to those corresponding to an energy of $148.8n^3$ Joules in terms of the initial elastic phase and the subsequent force plateau. Following this plateau, the load drops dramatically to another approximately constant plateau with its value just above zero, which is associated with fiction effect between the projectile and the composite panel after perforation. Similarly, impact damage under this type of loading condition is again dependent on scale size, as indicated in both the normalised traces, as shown in Figure 9b, and the damage morphology of the four scaled sizes of perforated panels, as shown in Figure 10. An examination of Figure 10 suggests that the failure mechanisms are similar at all scale sizes, with fibre fracture being predominant in all scales. However, there is evidence of matrix crushing failure in all scales and some delamination in the two larger scales. In spite of this, it is surprising to see how similar the perforation zones are in the four scaled sizes.

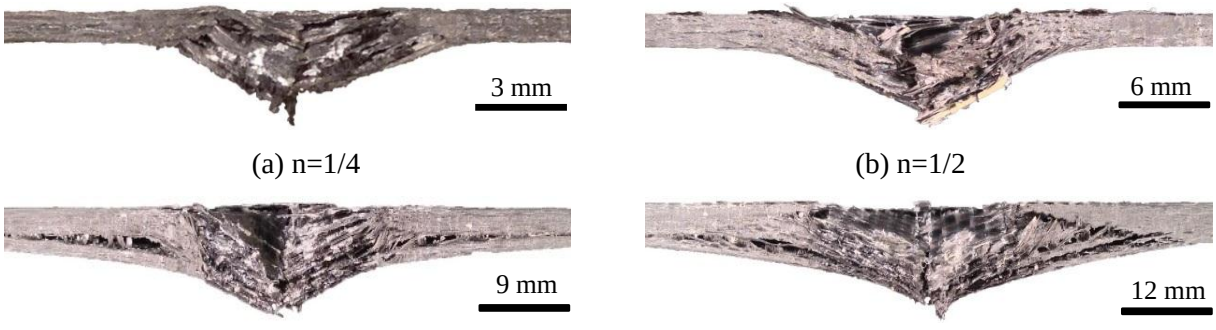

(a) n=1/4 (b) n=1/2

(c) n=3/4 (d) n=1

Figure 10: Damage morphology of the perforated panels after taking out the projectiles

To quantify the severity of impact damage, the effective projectile displacement associated with the fibre fracture phase was measured on each normalised trace and the resulting data are shown in Figure 11. Although there is some scatter in these data, particularly at the two intermediate impact energies, this fibre fracture phase exhibits a significant dependency on scale size, with its length increasing rapidly

with scale size. For example, for the lowest impact energy ($67.46n^3$ Joules), this region increases from approximately 2.5 mm to 9.5 mm in going from the smallest scale to the full scale, suggesting that damage should be more severe in larger panels. Interestingly, the scaled length values (except for the smallest scale) for the impact energy of $170.7n^3$ Joules are less than those for the impact energy of $148.8n^3$ Joules. It is believed that the presence of reduced fibre fracture phase in the case of $170.7n^3$ Joules is attributed to that some amount of this impact energy was absorbed by the development of delamination and matrix crushing failure, as shown in Figure 10, leading to a reduced projectile displacement needed for the fibre fracture phase.

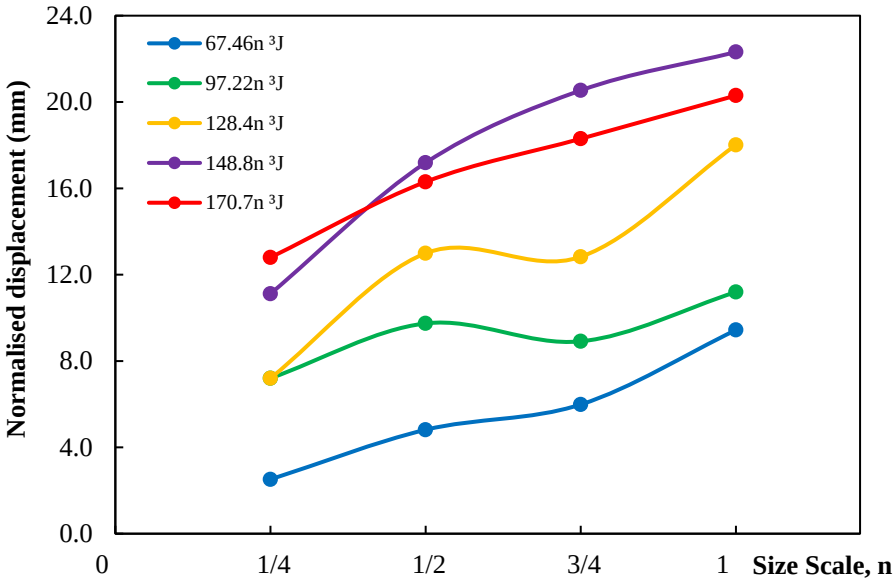

Figure 11: Variation of the normalised displacement in the fibre fracture phase with scale size

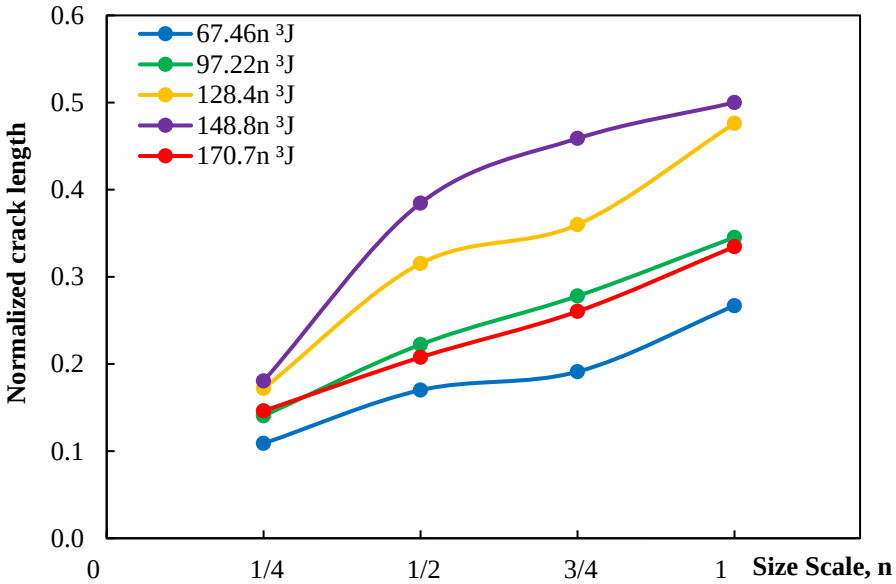

Figure 12: Variation of the normalised crack length with respect to scale size

The effect of increased severity of damage in the larger panels can also be characterised by measuring the total crack length in both the warp and weft directions on the rear surface and then normalising it to twice the panel length. Figure 12 shows the variation of the normalised crack length with respect to scale size. As is evident in this figure, the variations of the normalised crack length for all five impact energies

show similar trends, with the crack length increasing notably with scale size. For instance, for the impact energy of $148.8n^3$ Joules, the normalised crack length increases for almost three times from 0.18 at the smallest scale to 0.5 at the largest scale, again suggesting that damage is more severe in the large panels. It is also clear that for the lower four energies, the normalised crack length increases with increasing impact energy. However, compared to the results of the case of $148.8n^3$ Joules, the normalised crack lengths of the case of $170.7n^3$ Joules, which is an energy greater than that required to perforate the composite panels, decrease significantly at all the four scales. This effect, i.e. a higher impact energy producing shorter cracks in the scaled panels, is again believed to a result of that some amount of this impact energy was absorbed by the development of delamination and matrix crushing failure, mitigating the need of developing longer cracks in the fibre fracture phase under this impact condition.

It should be noted that the physical widths of the cracks in the warp and weft directions were similar in all scaled sizes of specimen as the cracks were constrained by adjacent tows and could not propagate laterally, as indicated in Figure 10. Knowing this, for a given impact energy either lower or higher than the perforation energy threshold, the effect of increased severity of damage in the larger panels also be explained from an energy point of view. Specifically, the amount of energy required to create fibre fracture, which is jointly determined by the total area of fracture that is created and the fracture energy associated with this failure mode, can be estimated from:

$$E_f = hl\gamma \tag{2}$$

where γ denotes the fracture energy density associated with this fibre-dominated failure mode, i.e. fibre fracture, and h and l represent the thickness of specimen and the length of fibre fracture, respectively. As γ is an intrinsic material property and independent of scale size, this energy term scales as n^2, rather than n^3, as is the case for the input energy. During the impact event, the elastic energy absorbing capability (a parameter that scales as n^3) has been surpassed, an additional amount of energy must be absorbed in failure mechanisms, primarily through further propagation of fibre fracture, as observed in the tested panels. Given that the energy absorbed in the fibre fracture process and the incident energy scale differently, it is argued that larger areas of fibre fracture are required to absorb the 'additional' amount of energy associated with perforation on larger specimens.

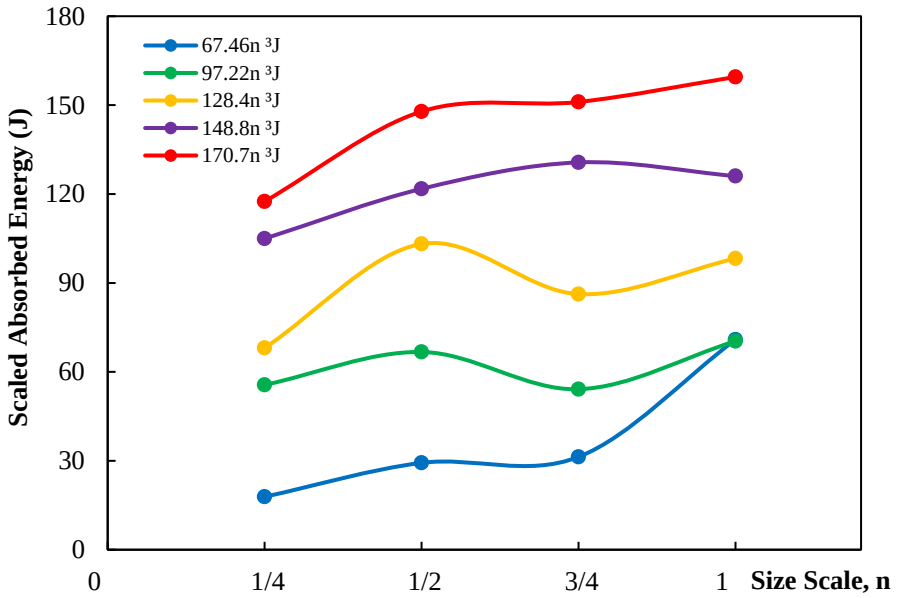

Figure 13: Variation of the scaled absorbed energy with respect to scale size

The evidence presented in Figures 11 and 12 clearly suggests that impact damage in these laminates does not obey a simple scaling law, with damage becoming more severe as scale size is increased. The energy absorbed during the impact event for each scale size and each impact energy was calculated as

the area under the normalised load-displacement trace, and the variation of this scaled energy with scale size is shown in Figure 13. Although there is some scatter in the trends in the energies associated with the intermediate scale sizes under impact loading, the data suggest that the absorbed energy increases with scale size. Looking at the scaled load-displacement traces presented above, it is evident that the extended regions associated with the fibre fracture phases in the larger samples lead to a significant increase in the maximum displacement and greater energy absorption, as evidenced by the area under the traces.

It is worth noting that the energies absorbed corresponding to the impact energy of 170.7 n^3 Joules were higher than those corresponding to the impact energy of 148.8 n^3 Joules, despite the former having lower projectile displacements in the fibre fracture phases and shorter cracks. Given that the absorbed energy associated with fibre fracture can be estimated using Eq. (2) and that shorter cracks absorb less energy than longer cracks, it is confirmed that under the impact energy of 170.7 n^3 Joules, this energy was absorbed through not only the formation of fibre fracture but also the development of delamination and matrix crushing failure, as evidenced in Figure 10.

5 CONCLUSIONS

Scaling effects in the low velocity impact response of plain woven CFRP composite laminates have been investigated based on experimental tests conducted at five different impact energies. It has been highlighted that the primary failure mechanism in these impacted panels was fibre fracture extending away from the centre of the panel and no significant delamination was observed. By analysing the normalised load-displacement data, it has been shown that the elastic response of the composite plates follows a simple scaling law. In contrast, impact damage does not scale in accordance with that predicted by simple scaling laws, with damage becoming more severe in the larger panels. It is argued that the energy absorbed in fibre fracture scales as the square of the scaling factor, i.e. n^2, whereas the incident energy scales as n^3. This discrepancy results in increased levels of energy being absorbed in fibre fracture mechanisms and severer damage in the larger panels. It has also been noted that at the impact energy higher than the perforation energy threshold, the failure mechanism of developing longer cracks as impact energy is increased, which would otherwise be required at impact energies lower than this energy threshold, was partially replaced by developing matrix crushing failure and interlaminar delamination, resulting in a reduced level of fibre fracture in the scaled panels subjected to this impact energy.

ACKNOWLEDGEMENTS

The lead author, Z.W. Xu, gratefully acknowledges the financial support from the China Scholarship Council (CSC) under grant number 201408060025.

REFERENCES

[1] L. S. Sutherland, R. A. Shenoi, and S. M. Lewisc, "Size and scale effects in composites: I. Literature review," *Composites Science and Technology*, vol. 59, pp. 209-220, 1999.

[2] M. R. Wisnom, "Scaling effects in the testing of fibre-composite materials," *Composites Science and Technology*, vol. 59, pp. 1937-1957, 1999.

[3] E. Buckingham, "On Physically Similar Systems; Illustrations of the Use of Dimensional Equations," *Physics Reviews*, vol. 4, pp. 345-376, 1914.

[4] M. R. Wisnom, "The effect of specimen size on the bending strength of unidirectional carbon fibre-epoxy," *Composite Structures*, vol. 18, pp. 47-63, 1991.

[5] S. Kellas and J. Morton, "Strength scaling in fiber composites," *AIAA Journal*, vol. 30, pp. 1074-1080, 1992.

[6] K. E. Jackson, S. Kellas, and J. Morton, "Scale Effects in the Response and Failure of Fiber Reinforced Composite Laminates Loaded in Tension and in Flexure," *Journal of Composite Materials*, vol. 26, pp. 2674-2705, 1992.

[7] D. P. Johnson, J. Morton, S. Kellas, and K. E. Jackson, "Size Effects in Scaled Fiber Composites Under Four-Point Flexure Loading," *AIAA Journal*, vol. 38, pp. 1047-1054, 2000.

[8] B. G. Green, M. R. Wisnom, and S. R. Hallett, "An experimental investigation into the tensile strength scaling of notched composites," *Composites Part A: Applied Science and Manufacturing*, vol. 38, pp. 867-878, 2007.

[9] M. R. Wisnom, S. R. Hallett, and C. Soutis, "Scaling Effects in Notched Composites," *Journal of Composite Materials*, vol. 44, pp. 195-210, 2009.

[10] G. H. Erçin, P. P. Camanho, J. Xavier, G. Catalanotti, S. Mahdi, and P. Linde, "Size effects on the tensile and compressive failure of notched composite laminates," *Composite Structures*, vol. 96, pp. 736-744, 2013.

[11] X. Xu, M. R. Wisnom, X. Li, and S. R. Hallett, "A numerical investigation into size effects in centre-notched quasi-isotropic carbon/epoxy laminates," *Composites Science and Technology*, vol. 111, pp. 32-39, 2015.

[12] J. Serra, C. Bouvet, B. Castanié, and C. Petiot, "Scaling effect in notched composites: The Discrete Ply Model approach," *Composite Structures*, vol. 148, pp. 127-143, 2016.

[13] K. Tang, H. Bao, and G. Liu, "Simulation on size effect of notched quasi-isotropic composite laminates under tensile loading," *Journal of Reinforced Plastics and Composites*, vol. 35, pp. 1623-1633, 2016.

[14] J. Morton, "Scaling of impact-loaded carbon-fiber composites," *AIAA Journal*, vol. 26, pp. 989-994, 1988.

[15] S. R. Swanson, "Scaling of impact damage in fiber composites from laboratory specimens to structures," *Composite Structures Volume*, vol. 25, pp. 249-255, 1993.

[16] J. Carrillo and W. Cantwell, "Scaling effects in the tensile behavior of fiber-metal laminates," *Composites Science and Technology*, vol. 67, pp. 1684-1693, 2007.

[17] J. G. Carrillo and W. J. Cantwell, "Scaling Effects in the Low Velocity Impact Response of Fiber-Metal Laminates," *Journal of Reinforced Plastics and Composites*, vol. 27, pp. 893-907, 2008.

[18] S. McKown, W. J. Cantwell, and N. Jones, "Investigation of Scaling Effects in Fiber--Metal Laminates," *Journal of Composite Materials*, vol. 42, pp. 865-888, 2008.

[19] F. J. Yang, M. Z. Hassan, W. J. Cantwell, and N. Jones, "Scaling effects in the low velocity impact response of sandwich structures," *Composite Structures*, vol. 99, pp. 97-104, 2013.

[20] Z. Xu, F. Yang, Z. W. Guan, and W. J. Cantwell, "An experimental and numerical study on scaling effects in the low velocity impact response of CFRP laminates," *Composite Structures*, vol. 154, pp. 69-78, 2016.

[21] Gurit. (2017). *DATASHEET / EP 121 - Epoxy Prepreg* Available: http://www.gurit.com/-/media/Gurit/Datasheets/ep-121pdf.ashx